

Development of CaMoO_4 crystal scintillators for double beta decay experiment with ^{100}Mo

A.N. Annenkov^a, O.A. Buzanov^a, F.A. Danevich^{b,1},
 A.Sh. Georgadze^b, S.K. Kim^c, H.J. Kim^d, Y.D. Kim^e,
 V.V. Kobychhev^b, V.N. Kornoukhov^f, M. Korzhik^g, J.I. Lee^e,
 O. Missevitch^g, V.M. Mokina^b, S.S. Nagorny^b,
 A.S. Nikolaiko^b, D.V. Poda^b, R.B. Podviyanuk^b, D.J. Sedlak^b,
 O.G. Shkulkova^b, J.H. So^d, I.M. Solsky^h, V.I. Tretyak^b,
 S.S. Yurchenko^b

^a*Moscow Steel and Alloy Institute, 119049, Moscow, Russia*

^b*Institute for Nuclear Research, MSP 03680 Kyiv, Ukraine*

^c*DMRC and School of Physics, Seoul National University, Seoul, 151-742,
 Republic of Korea*

^d*Physics Department, Kyungpook National University, Daegu, 702-701, Republic
 of Korea*

^e*Sejong University, Seoul, Republic of Korea*

^f*Institute for Theoretical and Experimental Physics, 117218 Moscow, Russia*

^g*Institute for Nuclear Problems, 220030 Minsk, Belarus*

^h*Institute for Materials, 79031 Lviv, Ukraine*

Abstract

Energy resolution, α/β ratio, pulse-shape discrimination for γ rays and α particles, temperature dependence of scintillation properties, and radioactive contamination were studied with CaMoO_4 crystal scintillators. A high sensitivity experiment to search for $0\nu 2\beta$ decay of ^{100}Mo by using CaMoO_4 scintillators is discussed.

Key words: Double beta decay, Scintillation detector, CaMoO_4 crystals,
 Pulse-shape discrimination, Radiopurity

PACS: 23.40.-s, 29.40.Mc

¹ Corresponding author. Address: Institute for Nuclear Research, Prospect Nauky 47, MSP 03680 Kyiv, Ukraine; tel: +380-44-525-1111; fax: +380-44-525-4463; E-mail address: danevich@kinr.kiev.ua

1 INTRODUCTION

As it was already demonstrated by several experiments, scintillation method is a promising tool to search for the double beta (2β) decay processes [1,2,3,4,5,6,7,8,9]. Scintillation detectors possess a range of important characteristics for a high sensitivity 2β decay experiment: high registration efficiency for 2β processes, reasonable energy resolution, pulse-shape discrimination ability to reduce background, operating stability, low cost. There exists a few detectors containing Molybdenum. The most promising of them, from the point of view of light output, is calcium molybdate (CaMoO_4). In Ref. [10] CaMoO_4 crystal scintillators were proposed to search for neutrinoless (0ν) double beta decay of ^{100}Mo . Recently CaMoO_4 was intensively studied as possible cryogenic scintillation-bolometric detector for experiments to search for 2β decay and dark matter [11,12,13,14,15,16].

^{100}Mo is one of the most promising candidate for 2β decay experiments because of its high transition energy ($Q_{2\beta}=3035$ keV). As a result, the calculated value of the phase space integral $G_{mm}^{0\nu}$ of the $0\nu 2\beta$ decay of ^{100}Mo is one of the largest among 35 possible $2\beta^-$ decay candidates [17,18]. Theoretical predictions for the product of half-life with the effective neutrino mass $T_{1/2}^{0\nu} \cdot \langle m_\nu \rangle^2$ are in the range of 8.0×10^{22} to 4.1×10^{24} yr·eV² (see compilations [19] and more recent calculations [20])². Moreover, from the experimental point of view, the larger is the $Q_{2\beta}$ energy, the simpler is to overcome background problems, in particular, because background from natural radioactivity drops sharply above 2615 keV, the energy of γ 's from ^{208}Tl decay (^{232}Th family). In addition, cosmogenic activation, which is important for the next generation 2β decay experiments (see, for instance [22]), contributes less at higher energies.

Two neutrino double beta decay ($2\nu 2\beta$) of ^{100}Mo to the ground state of ^{100}Ru was already observed in a few direct experiments [23] with measured half-lives in the range of $3.3 \times 10^{18} - 1.2 \times 10^{19}$ yr; the most exact value comes from the recent measurements in the NEMO-3 experiment as $T_{1/2} = 7.1 \pm 0.5 \times 10^{18}$ yr [24]. Geochemical measurements gave the value of $T_{1/2} = 2.2 \pm 0.3 \times 10^{18}$ yr [25]. In addition to transition to the ground state, also $2\nu 2\beta$ decay of ^{100}Mo to the first excited 0_1^+ level of ^{100}Ru ($E_{exc} = 1131$ keV) was observed; measured values of half-lives are in the range of $(5.7 - 9.3) \times 10^{20}$ yr [26]. The neutrinoless 2β decay still is not observed: the highest limit was reached in the NEMO-3 experiment as $T_{1/2} > 4.6 \times 10^{23}$ yr at 90% C.L. [24].

The purpose of our work was investigation of energy resolution, light yield, α/β ratio, pulse shape for γ rays and α particles, temperature dependence of scintillation properties, pulse-shape discrimination ability with a few samples

² One very deviating result is also known: 3.6×10^{27} yr·eV² in accordance with [21].

Table 1
 Properties of CaMoO_4 , CaWO_4 , and CdWO_4 crystal scintillators.

	CaMoO_4	CaWO_4	CdWO_4
Density (g/cm^3)	4.2	6.1	8.0
Melting point ($^\circ\text{C}$)	1430	1570 – 1650	1325
Structural type	Scheelite	Scheelite	Wolframite
Cleavage plane	Weak (001)	Weak (101)	Marked (010)
Hardness (Mohs)	3.5 – 4	4.5 – 5	4 – 4.5
Wavelength of emission maximum (nm)	520	420 – 440	480
Refractive index	1.98	1.94	2.2 – 2.3
Effective average decay time* (μs)	14	8	13
Photoelectron yield [% of NaI(Tl)]*	9%	18%	20%

*For γ rays, at room temperature.

of CaMoO_4 crystal scintillators produced by the Institute for Materials (IM, Lviv, Ukraine), and by the Innovation Centre of the Moscow Steel and Alloy Institute (ICMSAI, Moscow, Russia). Radioactive contamination of four samples of CaMoO_4 crystals was tested in the Solotvina Underground Laboratory.

2 SAMPLES

The main properties of CaMoO_4 scintillators are presented in Table 1, where characteristics of calcium and cadmium tungstates are also given for comparison. The material is non-hygroscopic and chemically resistant. Five clear, practically colorless CaMoO_4 crystals were used in our studies. The crystals were fabricated from single crystals grown by the Czochralski method. All crystals used in the present study are listed in Table 2.

3 MEASUREMENTS AND RESULTS

3.1 Energy resolution

In the present work, the energy resolution was measured for all the CaMoO_4 samples.

The CaMoO_4 crystal (CMO-4) was diffused at the side surface with the help

Table 2

Samples of CaMoO_4 crystal scintillators used in this study, and their scintillation properties.

ID	Size (mm)	Mass (g)	Manufac- turer	Relative pulse amplitude	FWHM at 662 keV
CMO-1	$25 \times 13 \times 9$	11.5	IM ^a	100%	12.8% ^c
CMO-2	$\varnothing 38 \times 20$	95.6	IM ^a	103%	12.5% ^d
CMO-3	$\varnothing 38 \times 20$	99.9	IM ^a	110%	11.9% ^d
CMO-4	$\varnothing 38 \times 20$	97.8	IM ^a	118%	10.3% ^d
CMO-5	$28 \times 28 \times 24$	82.5	ICMSAI ^b	79%	14.0% ^c

^a Institute for Materials (Lviv, Ukraine)

^b Innovation Centre of the Moscow Steel and Alloy Institute (Moscow, Russia)

^c exit surface (coupled to PMT) was polished; other surfaces were diffused

^d exit and opposite surfaces were polished; side surface was diffused

of fine grinding paper, the exit and top surfaces were polished. The scintillator was wrapped by PTFE reflector tape and optically coupled to 3" photomultiplier (PMT) Philips XP2412. The measurements were carried out with the help of the home-made spectroscopy amplifier with 16 μs shaping time to collect most of the charge from the anode of the PMT. The scintillator was irradiated by γ quanta of ^{137}Cs , ^{207}Bi , ^{232}Th , and ^{241}Am sources. The energy resolutions (full width at half maximum, FWHM) of 34% (^{241}Am , 60 keV), 10.3% (^{137}Cs , 662 keV), 7.7% (^{207}Bi , 1064 keV), and 4.7% (^{208}Tl , 2615 keV) were measured (see Fig. 1). The energy resolution obtained in the present study is the best ever reported for CaMoO_4 crystal scintillators. It is important to stress that the clear peak of 2615 keV γ line of ^{208}Tl (^{232}Th source) was accumulated with the energy resolution of 4.7%. It demonstrates a possibility to calibrate the energy scale of a CaMoO_4 detector in the vicinity of the expected peak of $0\nu 2\beta$ decay of ^{100}Mo with the help of a ^{228}Th source.

Dependence of energy resolution and light output on surface treatment was checked with the sample CMO-5. First, all surfaces of the crystal were polished. The crystal was wrapped by three layers of PTFE tape and optically connected to PMT XP2412. The spectroscopy amplifier with 16 μs shaping time was used. The energy resolution of 16.2% was measured in this conditions for ^{137}Cs 662 keV γ line. Then surface of the crystal, except of exit window connected to the PMT, was diffused by fine-grained grinding paper. The relative pulse amplitude was increased at 1.21 times and the energy resolution was improved to 14.0%.

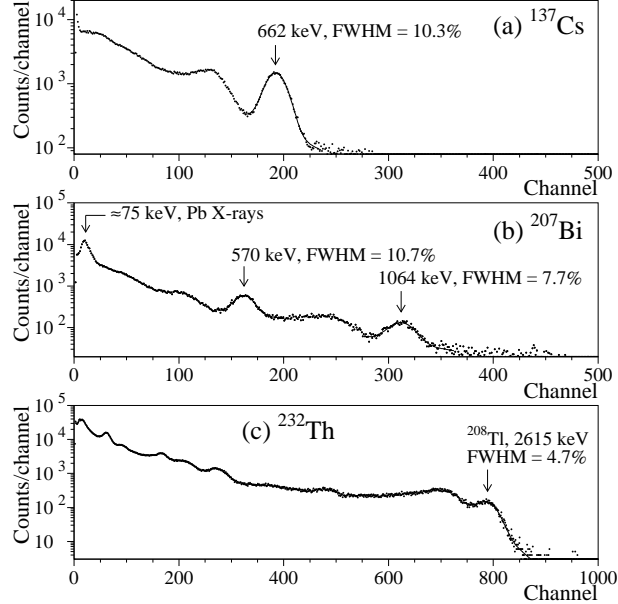


Fig. 1. Energy spectra of ^{137}Cs (a), ^{207}Bi (b), and ^{232}Th (c) γ quanta measured with CaMoO_4 scintillation crystal $\varnothing 38 \times 20$ mm (CMO-4).

3.2 Light yield

The relative photoelectron yield of the CaMoO_4 crystal (CMO-4) was measured relatively to the CaWO_4 scintillator $\varnothing 40 \times 39$ mm described in [27]. The crystals were coupled to PMT XP2412 with the bialkali photocathode and were irradiated by γ quanta of ^{137}Cs source. The spectroscopy amplifier with the shaping time $16 \mu\text{s}$ was used in this test. The relative photoelectron yield of the CaMoO_4 scintillator was measured as 36% of the CaWO_4 .

Photoelectron yield of the CMO-4 scintillator was also measured relatively to the $\text{NaI}(\text{Tl})$ scintillator $\varnothing 40 \times 40$ mm of standard assembling. To avoid an effect of the substantial difference in the scintillation decay of CaMoO_4 ($14 \mu\text{s}$) and $\text{NaI}(\text{Tl})$ ($0.25 \mu\text{s}$), the energy spectra were built by calculating areas of pulses (over $300 \mu\text{s}$ for CaMoO_4 and $6 \mu\text{s}$ for $\text{NaI}(\text{Tl})$) accumulated with the help of 20 MS/s transient digitizer based on the 12 bit ADC (AD9022) [28]. The photoelectron yield of 8% relatively to $\text{NaI}(\text{Tl})$ was obtained for the CMO-4 sample.

3.3 α/β ratio

The α/β ratio was measured with the CMO-1 crystal by using collimated α particles of a ^{241}Am source. The dimensions of the collimator were $\varnothing 0.75 \times 2$ mm. As it was checked by a surface-barrier detector, the energy of α particles

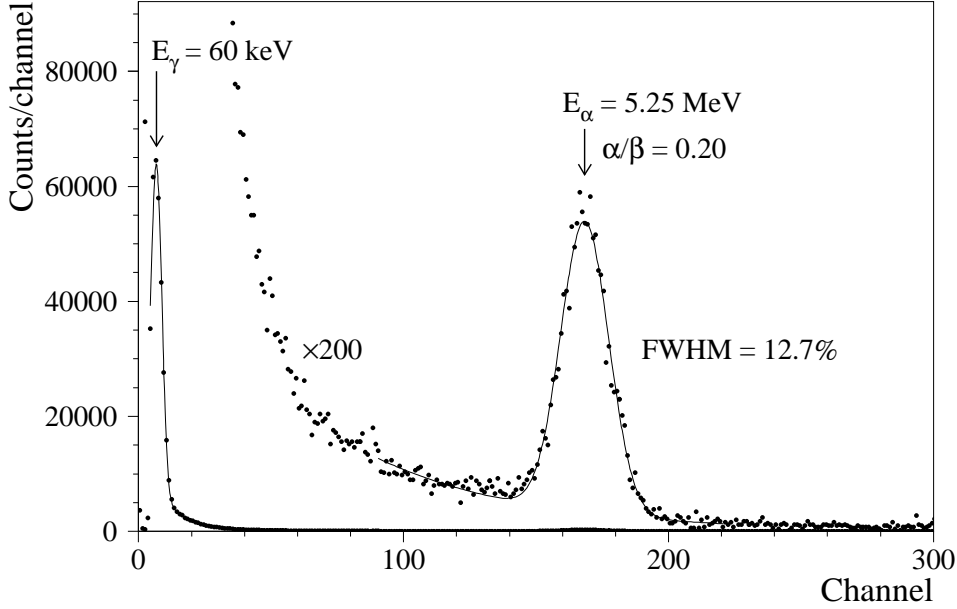


Fig. 2. The energy spectrum measured with 5.25 MeV α particles from ^{241}Am source (dots). Fits of α and 60 keV γ peaks are shown by solid lines.

was reduced to about 5.25 MeV by 2 mm of air due to passing through the collimator [29]. Fig. 2 shows the energy spectrum of the α particles measured by the CaMoO_4 scintillator. The α/β ratio is 0.20 at the energy of α particles 5.25 MeV.

Besides the measurements with the external source, α peaks of ^{220}Rn and ^{216}Po (from ^{232}Th chain), ^{210}Po and ^{214}Po (^{238}U), presented in trace amount in the CaMoO_4 crystal ($\varnothing 38 \times 20$ mm, CMO-2), were used to extend the energy range of α particles. The peaks of ^{220}Rn , ^{216}Po and ^{214}Po were selected with the help of the time-amplitude analysis of data obtained in the low background measurements (see subsection 3.7.3). The clear peak of ^{210}Po is presented in the energy spectrum of CaMoO_4 detector (subsection 3.7.2). The measured dependence of the α/β ratio on energy of α particles (Fig. 3) can be described in the energy region 5–8 MeV by the linear function: $\alpha/\beta = 0.11(2) + 0.019(3)E_\alpha$, where E_α is energy of α particles in MeV.

3.4 Pulse shape for γ rays and α particles

Pulse shape of CaMoO_4 scintillator (CMO-1) was studied with the help of the 12 bit transient digitizer operated at 20 MS/s. To study pulse shape of scintillation decay for α particles, the CaMoO_4 crystal was irradiated by α particles from collimated ^{241}Am source. A ^{60}Co source was used to investigate pulse shape for γ quanta. Measurements were carried out at the temperature $(27 \pm 1)^\circ\text{C}$.

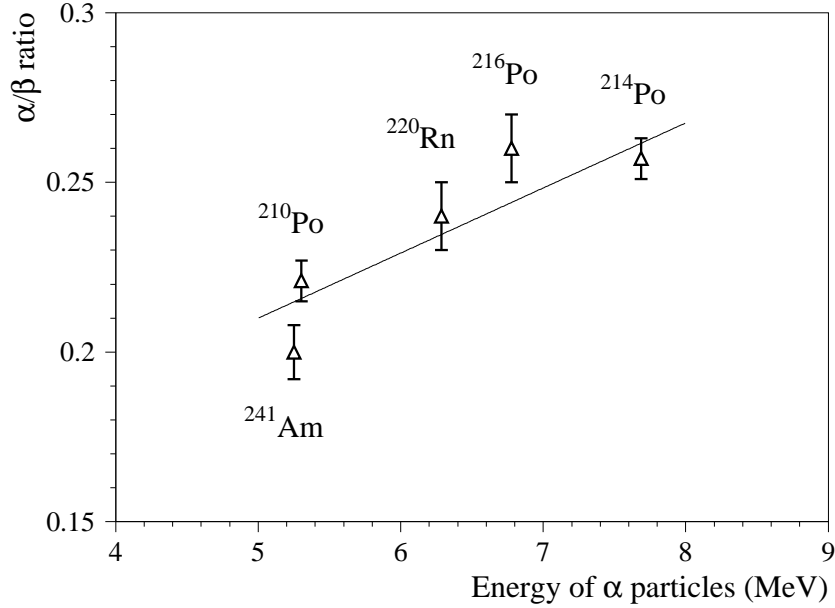


Fig. 3. Dependence of α/β ratio for CaMoO_4 scintillator on energy of α particles.

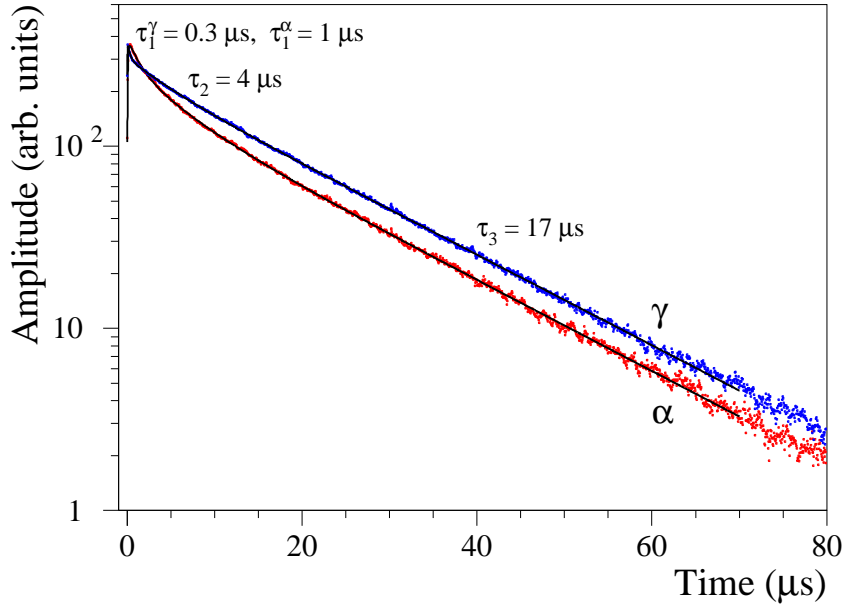


Fig. 4. Decay of scintillation in CaMoO_4 crystal for γ rays and α particles measured by 20 MS/s transient digitizer. Three components of scintillation signals with time decay of 0.3–1 μs , 4 μs and 17 μs are shown. Fitting functions for α and γ pulses are shown by solid lines.

The shape of the light pulses produced by α particles and γ rays in the CaMoO_4 scintillator measured by the 20 MS/s digitizer are shown in Fig. 4. To obtain the pulse shapes, about one thousand of individual α (γ) events with amplitudes corresponding to α peak of ^{241}Am were summed. The pulses were fitted by the function:

Table 3

Decay time of CaMoO_4 scintillators for γ quanta and α particles measured by 20 MS/s transient digitizer at the temperature $+27^\circ\text{C}$. The decay constants and their relative intensities are denoted as τ_i and A_i , respectively.

Type of irradiation	Decay constants and relative intensities		
	τ_1 (A_1)	τ_2 (A_2)	τ_3 (A_3)
α particles	1 μs (2%)	4 μs (13%)	17 μs (85%)
γ rays	0.3 μs (0.5%)	4 μs (5.5%)	17 μs (94%)

$$f(t) = \sum A_i(e^{-t/\tau_i} - e^{-t/\tau_0})/(\tau_i - \tau_0), \quad t > 0,$$

where A_i are the relative intensities, τ_i are the decay constants for different light-emission components, and τ_0 is integration constant of electronics ($\tau_0 \approx 0.08 \mu\text{s}$). Three decay components were observed with $\tau_i \approx 0.3 - 1 \mu\text{s}$, $\approx 4 \mu\text{s}$, and $\approx 17 \mu\text{s}$ with different intensities for γ rays and α particles (see Fig. 4 and Table 3).

3.5 Pulse-shape discrimination between γ rays and α particles

The difference of the pulse shapes allows to discriminate $\gamma(\beta)$ events from those induced by α particles. We applied for this purpose the optimal filter method proposed in [30], and successfully used for different scintillation detectors: CdWO_4 [28,31], CeF_3 [7], CaWO_4 [27], YAG:Nd [32], ZnWO_4 [9], $\text{CaF}_2(\text{Eu})$ [33], PbWO_4 [34]. For each CaMoO_4 signal, a numerical characteristic (shape indicator, SI) was calculated in the following way:

$$SI = \sum f(t_k)P(t_k) / \sum f(t_k),$$

where the sum is over time channels k , starting from the origin of pulse and up to $50 \mu\text{s}$, $f(t_k)$ is the digitized amplitude (at the time t_k) of the signal. The weight function $P(t)$ was defined as: $P(t) = \{f_\alpha(t) - f_\gamma(t)\} / \{f_\alpha(t) + f_\gamma(t)\}$, where $f_\alpha(t)$ and $f_\gamma(t)$ are the reference pulse shapes for α particles and γ quanta.

Reasonable discrimination between α particles and γ rays was achieved using this approach, as one can see in Fig. 5 where the SI distributions measured with the CaMoO_4 scintillation crystal CMO-1 for α particles ($E_\alpha \approx 5.25 \text{ MeV}$) and γ quanta ($\approx 1 \text{ MeV}$) are shown. As a measure of discrimination ability (factor of merit, FOM), the following expression can be used:

$$FOM = |SI_\alpha - SI_\gamma| / \sqrt{\sigma_\alpha^2 + \sigma_\gamma^2},$$

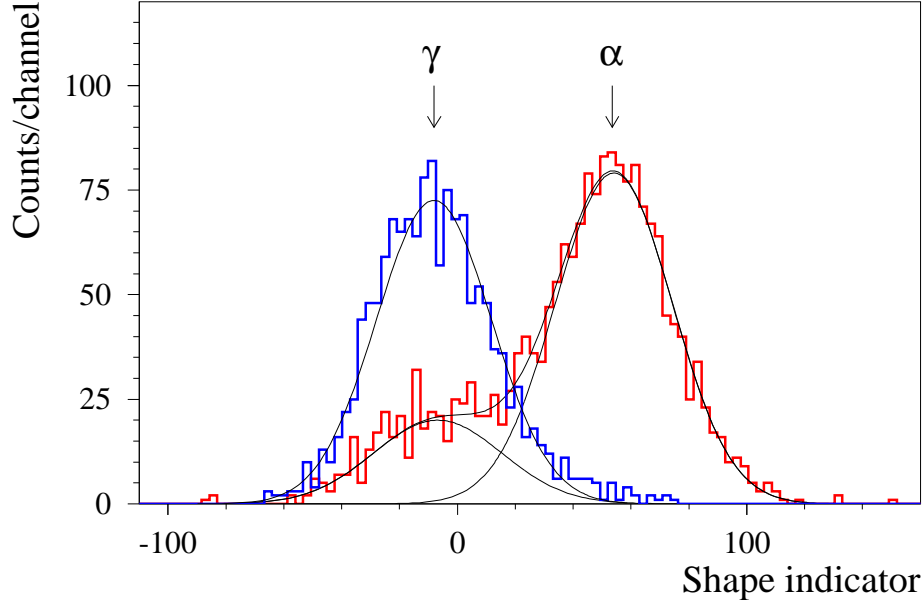


Fig. 5. The shape indicator (see text) distributions measured by CaMoO_4 detector with α particles ($E_\alpha = 5.25$ MeV) and γ quanta (≈ 1 MeV) using 20 MS/s 12 bit transient digitizer. The distributions were fitted by Gaussian function (solid lines). The small tail in the shape indicator distribution for α at ≈ -10 can be explained by background γ events.

where SI_α and SI_γ are mean SI values for α particles and γ quanta distributions (which are well described by Gaussian functions), σ_α and σ_γ are the corresponding standard deviations. For the distributions presented in Fig. 5, the factor of merit $FOM = 2.2$.

3.6 Temperature dependence of light output and pulse shape

Temperature dependence of scintillation properties were studied in the range of $-158 \div +25$ °C with the CMO-1 sample. The crystal was viewed by PMT XP2412 through a high purity quartz light-guide 4.9 cm in diameter and 25 cm long. The CaMoO_4 scintillator and the light-guide were wrapped by PTFE tape as reflector. Dow Corning Q2-3067 optical couplant was used to provide optical contact of the scintillator with the light-guide, and of the light-guide with the PMT. The crystal and main part of the light-guide were placed into a Dewar vessel, while PMT was isolated from the vessel with the help of a foam plastic plate. In such a way the temperature of PMT was kept stable (practically at room temperature) during the measurements. The Dewar vessel was periodically filled by small portions of liquid nitrogen to cool the detector. The temperature of the crystal was measured with the help of a chromel-alumel thermocouple.

To measure the relative light output and pulse shape, the scintillator was irradiated by α particles of the collimated ^{241}Am source ($E_\alpha = 5.25$ MeV). The 20 MS/s transient digitizer was used to accumulate four thousands scintillation pulse shapes of CaMoO_4 at each temperature. Then the recorded pulse shapes were used to build energy spectra and to determine the decay time. The energy spectra were obtained by calculation of the area of each signal from the starting point up to 380 μs .

To present behaviour of scintillation decay with temperature, we use the averaged decay time $\langle\tau\rangle$ determined by the following formula:

$$\langle\tau\rangle = \sum(\tau_i A_i) / \sum A_i.$$

The obtained dependence of averaged decay time on temperature is presented in Fig. 6 (a), and can be fitted in the temperature interval $-127 \div +25$ $^\circ\text{C}$ by the function $\langle\tau\rangle = 31.8(7) - 0.85(3) \times T + 0.0093(7) \times T^2$, where T is temperature in degree C. At the temperature -50 $^\circ\text{C}$ (where the maximum of light output was observed) the averaged decay time is ≈ 98 μs . The dependence of the averaged decay time on temperature for CaMoO_4 scintillator agrees qualitatively with the result reported in Ref. [10].

The measured dependence of relative light output of CaMoO_4 crystal scintillator on temperature is presented in Fig. 6 (b). The relative light output (*RLO*) increases with decreasing of the temperature down to ≈ -50 $^\circ\text{C}$ as $RLO = 1.374(16) - 0.0137(8) \times T - 0.00005(3) \times T^2$, where T is temperature in degrees C. Then some decrease of scintillation intensity was observed. The dependence is in agreement with the result obtained in Ref. [10].

Temperature dependence of the radioluminescence intensity was also studied with the help of photon counting method. The dependence was measured in the temperature range $-170 \div +40$ $^\circ\text{C}$ under gamma-excitation by ^{57}Co source. Light from sample was directed to the PMT (FEU-100) input window through a condenser. The ^{57}Co source was installed at 8 cm distance from the sample. PMT counting rate was averaged during 10 s at each value of the temperature. The dependence of the luminescence yield is presented in Fig. 7. It was found that at temperature decrease down to -80 $^\circ\text{C}$ the light yield increases by the factor of 2.5. Light yield remains practically unchanged at the further temperature decrease to -170 $^\circ\text{C}$.

The difference in the temperature dependence of light yield measured by two methods can be explained by considerable increase of the scintillation decay time at temperatures lower than ~ -50 $^\circ\text{C}$. Whereas result of the photon counting method (with time window 10 s) does not depend on the decay time, the relative light output obtained by using the transient digitizer (when scintillation pulses were integrated over 380 μs) depends on the kinetics of scintillation decay. After this effect was taken into account, the behaviour of

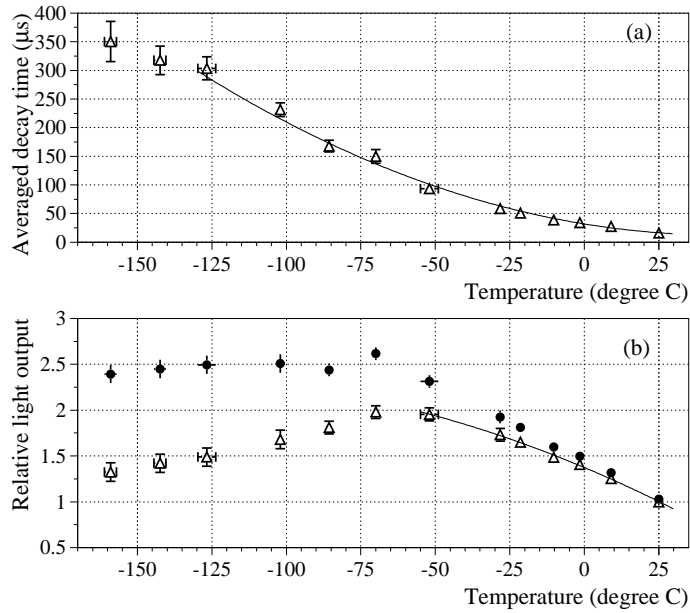


Fig. 6. (a) Temperature dependence of averaged decay time measured with CaMoO₄ detector under irradiation by α particles of ^{241}Am source. (b) The dependence of relative light output on temperature (triangles). The data corrected taking into account decay time of scintillation signals are shown by filled circles. Solid lines represent fits of the data.

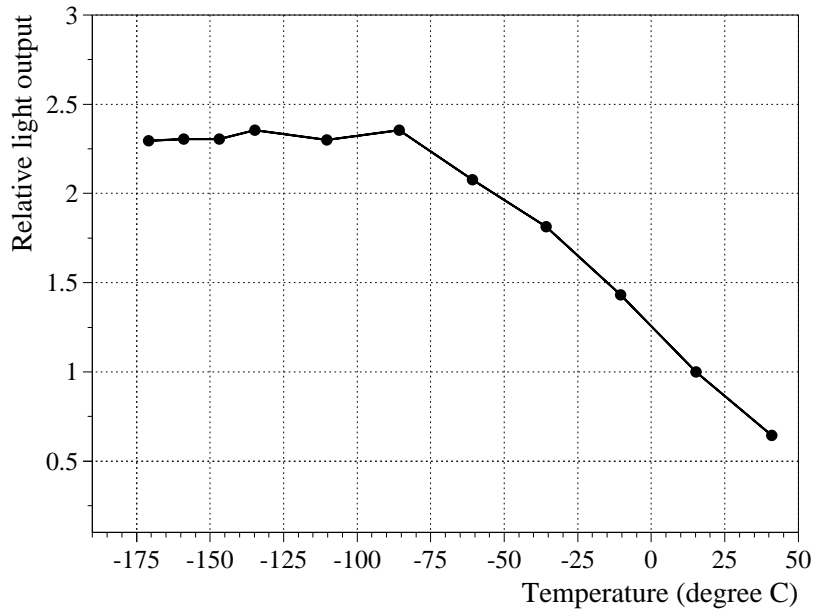


Fig. 7. Temperature dependence of radioluminescence intensity of CaMoO₄ crystal measured with the help of photon counting method.

the relative pulse amplitude measured with the digitizer (the corrected data are presented in Fig. 6 (b) by filled circles) are practically the same as measured with the help of the photon counting method.

3.7 Radioactive contamination

3.7.1 Set-up and measurements

Radiopurity of four samples (CMO–2, CMO–3, CMO–4, and CMO–5) was tested in the Solotvina Underground Laboratory built in a salt mine 430 m underground (≈ 1000 m of water equivalent) [35].

The crystals CMO–2, CMO–3, and CMO–4 were produced from one boule with aim to study a possible dependence of radioactive contamination on length of the boule. Such a dependence was observed for CdWO_4 crystals produced for the Solotvina experiment to search for 2β decay of ^{116}Cd [36]. The crystal CMO–2 was cut from the top of the boule (beginning of growth), the CMO–3 was taken from the middle part, and the CMO–4 sample was produced from the bottom part of the monocrystal boule.

Radioactive contamination of the CaMoO_4 crystals was measured in the low background set-up installed in the Solotvina Underground Laboratory. In the set-up a scintillation CaMoO_4 crystal was viewed by the special low-radioactive 5'' photomultiplier tube (EMI D724KFLB) through the high purity quartz light-guide $\varnothing 10 \times 33$ cm. The detector was surrounded by a passive shield made of teflon (thickness of 3–5 cm), plexiglass (6–13 cm), high purity (OFHC) copper (3–6 cm), lead (15 cm) and polyethylene (8 cm). For each event occurred in the detector, the amplitude of a signal and arrival time were recorded. In addition, CaMoO_4 scintillation pulse shapes were digitized with a 20 MHz sampling frequency in $\approx 100 \mu\text{s}$ full range. Energy scale of the detectors was calibrated with the help of ^{207}Bi γ source through the calibration channel made in the shield. For instance, the energy resolution of the CMO–2 crystal was $\text{FWHM} = 17.8\%$ and 13.5% for 570 and 1064 keV γ lines, respectively.

3.7.2 Interpretation of background spectrum

The energy spectrum of the CMO–2 detector measured during 74.83 h in the low background set-up is presented in Fig. 8. The peak at the energy ≈ 1.17 MeV can be attributed to intrinsic ^{210}Po (daughter of ^{210}Pb from the ^{238}U family) with activity of $0.42(1)$ Bq/kg. The equilibrium of the uranium chain in the crystal was broken during the crystal production, because there is no peak of ^{238}U expected at the energy of ≈ 0.82 MeV (in the gamma scale). Analysis of the spectrum gives only limit for activity of ^{238}U on the level of ≤ 0.5 mBq/kg. The same situation is with peaks of the uranium's daughters ^{234}U , ^{230}Th , and ^{226}Ra , which cannot be resolved (their Q_α values are very close). A common for these nuclides α peak is expected at the energy ≈ 1 MeV. Fit of the spectrum gives again only the limit for the total activity of

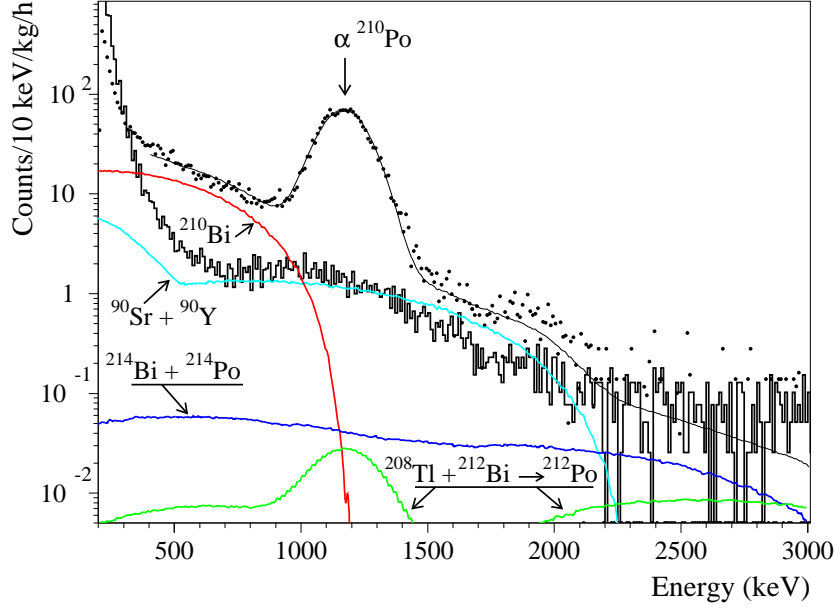


Fig. 8. Energy spectrum of CaMoO_4 scintillation crystal (CMO-2, dots) measured in the low background set-up during 74.83 h. Solid line represents the fit of the data by the background model in the 0.4 – 3 MeV energy interval. The peak with the energy ≈ 1.17 MeV is mainly due to the α decay of ^{210}Po . Most important components of the background (^{210}Bi , $^{90}\text{Sr}+^{90}\text{Y}$, $^{208}\text{Tl} + ^{212}\text{Bi} \rightarrow ^{212}\text{Po}$, and $^{214}\text{Bi} + ^{214}\text{Po}$) are shown. The spectrum measured during 472.4 h with the crystal CMO-5 in the same conditions is drawn by solid histogram. Both spectra are normalized on mass of the crystals and time of measurements.

these isotopes at the level of 2.8 mBq/kg. In the same way the following limits on the activities of ^{222}Rn , ^{218}Po , and ^{232}Th were obtained: ≤ 4.4 mBq/kg, ≤ 4.2 mBq/kg, and ≤ 0.7 mBq/kg, respectively.

To take into account presence in the crystal of β active isotopes (from U/Th families, ^{40}K , $^{90}\text{Sr}+^{90}\text{Y}$), the energy spectrum of the CaMoO_4 detector was simulated with the GEANT4 package [37]. Initial kinematics of particles emitted in β decays of nuclei was generated with the DECAY0 event generator [38]. The spectrum of the CMO-2 crystal (Fig. 8) was fitted in the energy interval 0.4 – 3 MeV by the model, which includes the simulated distributions of U/Th daughters (^{208}Tl and $^{212}\text{Bi} \rightarrow ^{212}\text{Po}$, ^{210}Bi , $^{214}\text{Bi} + ^{214}\text{Po}$, ^{234m}Pa), ^{40}K , $^{90}\text{Sr}+^{90}\text{Y}$, Gaussian function to describe the α peak of ^{210}Po , and an exponential function to take into account external γ background. The main components of the background are shown in Fig. 8. The major part of the β activity can be ascribed to ^{210}Bi , daughter of ^{210}Pb (≈ 0.4 Bq/kg). We cannot also exclude presence of significant activity of $^{90}\text{Sr}+^{90}\text{Y}$ in the crystal. Nevertheless, because there are no clear peculiarities which can be used to prove presence of these nuclides, we can give only the limit on activities of $^{90}\text{Sr}+^{90}\text{Y}$ and ^{210}Bi in the crystal at the level of ≤ 62 mBq/kg and ≤ 398 mBq/kg, respectively.

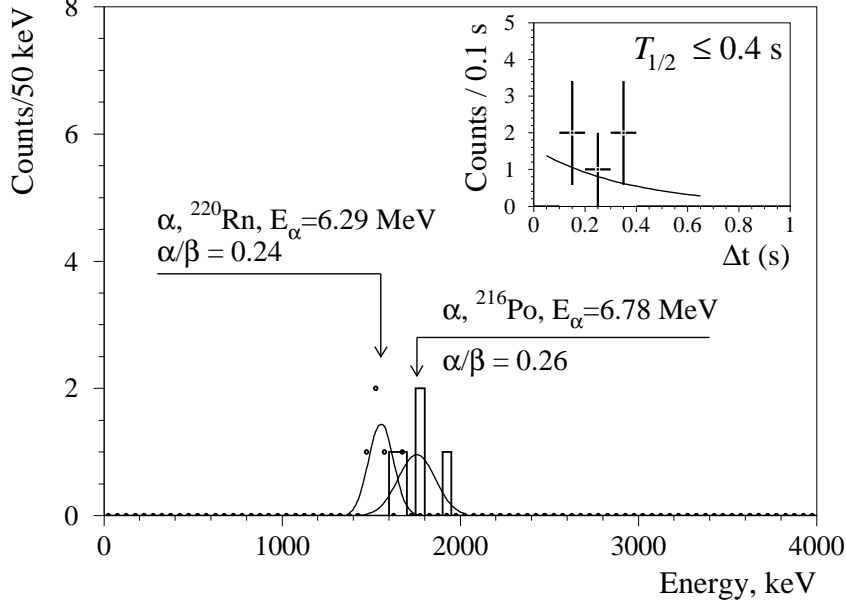


Fig. 9. The energy distributions for the fast sequence of the α decays of ^{220}Rn and ^{216}Po selected from the background data by the time-amplitude analysis. (Inset) The time distribution between the first and second events together with an exponential fit.

3.7.3 Time-amplitude analysis

The raw background data were analyzed by the time-amplitude method, when the energy and arrival time of each event were used for selection of some decay chains in ^{232}Th and ^{238}U families³. For instance, the following sequence of α decays from the ^{232}Th family was searched for and observed: ^{220}Rn ($Q_\alpha = 6.41$ MeV, $T_{1/2} = 55.6$ s) \rightarrow ^{216}Po ($Q_\alpha = 6.91$ MeV, $T_{1/2} = 0.145$ s) \rightarrow ^{212}Pb . These radionuclides are in equilibrium with ^{228}Th from ^{232}Th family. Because the energy of α particles from ^{220}Rn decay corresponds to $\simeq 1.5$ MeV in γ scale of the CaMoO_4 detector, the events in the energy region 1.4 – 2.2 MeV were used as triggers. Then all events (within 1.4 – 2.2 MeV) following the triggers in the time interval 0.02 – 0.6 s (containing 84% of ^{216}Po decays) were selected. The obtained α peaks (see Fig. 9) are in agreement with those expected for α particles of $^{220}\text{Rn} \rightarrow ^{216}\text{Po} \rightarrow ^{212}\text{Pb}$ chain [39]. The pulse-shape analysis confirms the nature of the events as caused by α particles. On this basis, in spite of low statistic, the activity of ^{228}Th in the CaMoO_4 crystal can be calculated as 0.23(10) mBq/kg.

Similarly, for the analysis of the ^{226}Ra chain (^{238}U family) the following sequence of β and α decays was used: ^{214}Bi ($Q_\beta = 3.27$ MeV) \rightarrow ^{214}Po ($Q_\alpha = 7.83$ MeV, $T_{1/2} = 164$ μs) \rightarrow ^{210}Pb . For the first event the lower energy threshold was set at 0.25 MeV, while for the events of the α decay of ^{214}Po the energy

³ Technique of a time-amplitude analysis of background data to recognize a presence of the short-living chains from ^{232}Th , ^{235}U and ^{238}U families was described in [36,5].

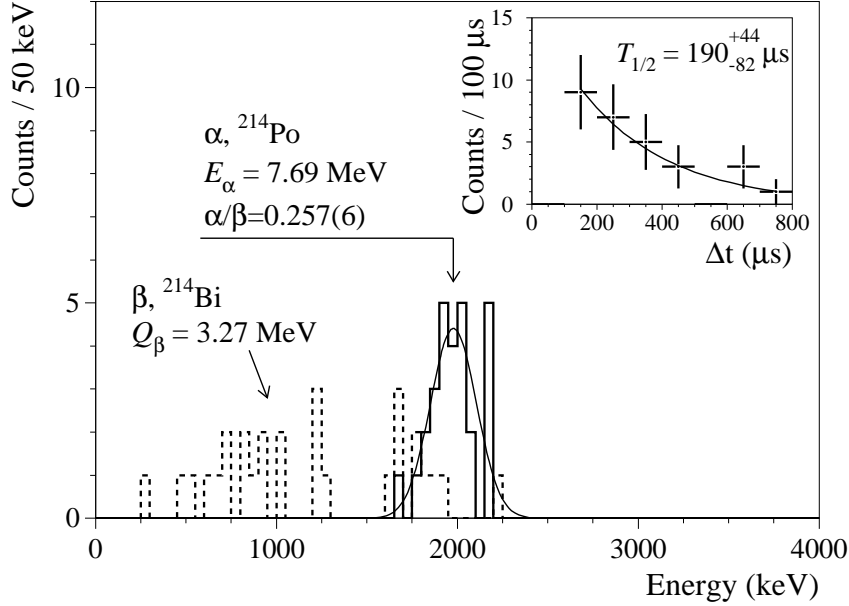


Fig. 10. The energy distributions for the fast sequence of the β (^{214}Bi) and α (^{214}Po) decays selected from the background data by the time-amplitude analysis. (Inset) The time distribution between the first and second events together with an exponential fit. The obtained half-life of ^{214}Po ($190^{+44}_{-82} \mu\text{s}$) is in agreement with the table value ($164 \mu\text{s}$) [39].

window 1.4 – 4 MeV was chosen. The events were selected in the time interval of 100 – 800 μs (55% of ^{214}Po decays). Taking into account the registration efficiency for events of ^{214}Bi with the energy threshold 0.25 MeV (85%), the obtained spectra (Fig. 10) lead to the ^{226}Ra activity in the CaMoO_4 crystal of 2.1(4) mBq/kg.

The results obtained with the help of time-amplitude analysis don't contradict the results of the analysis described in subsection 3.7.2 if one takes into account broken equilibrium of ^{232}Th and ^{238}U chains.

Estimation of radioactive contamination in other crystals was done in the same way as described above. The summary of the measured radioactive contamination of the CaMoO_4 scintillators (or limits on their activities) is given in Table 4, again in comparison with CaWO_4 [27] and CdWO_4 detectors [40,41,3,6].

One can see that radioactive impurities in the CaMoO_4 crystals are comparable with CaWO_4 crystals, and are much higher (by factor of 10 – 10^3) than those of the CdWO_4 scintillators. The radioactive contamination of CaMoO_4 crystal produced in the Innovation Centre of Moscow Steel and Alloy Institute is lower than that of the scintillators produced in the Institute for Materials. Some indication on increasing of radioactive contamination in the crystal volume during the growth process was observed with the samples CMO-2, CMO-3, and CMO-4 produced from the same crystal boule.

Table 4

Radioactive contaminations in CaMoO_4 , CaWO_4 , and CdWO_4 crystals scintillators.

Source	Activity (mBq/kg)					
	CMO-2	CMO-3	CMO-4	CMO-5	CaWO [27]	CdWO [40,41,3,6]
^{232}Th :						
^{232}Th	≤ 0.7	≤ 0.7	≤ 0.9	≤ 1.5	0.69(10)	0.053(5)
^{228}Th	0.23(10)	0.42(17)	0.4(4)	0.04(2)	0.6(2)	$\leq 0.004 - 0.039(2)$
^{238}U :						
^{238}U	≤ 0.5	≤ 0.6	≤ 0.6	≤ 1.5	5.6(5)	≤ 0.004
^{226}Ra	2.1(4)	2.5(5)	2.4(1.3)	0.13(4)	5.6(5)	≤ 0.004
^{210}Pb	≤ 398	≤ 401	≤ 550	≤ 17	≤ 430	≤ 0.4
^{210}Po	420(10)	490(10)	550(20)	≤ 8	291(5)	≤ 0.4
^{40}K	≤ 1.1	≤ 2.1	≤ 2.5	≤ 3	≤ 12	0.3(1)
^{90}Sr	≤ 62	≤ 178	≤ 50	≤ 23	≤ 70	≤ 0.2

4 High sensitivity ^{100}Mo $0\nu 2\beta$ experiment with CaMoO_4 detectors

Below we discuss possible use of CaMoO_4 scintillators as potential detectors in search for neutrinoless 2β decay of ^{100}Mo . Because of the "source=detector" approach (which provides high efficiency for detection of the process), good energy resolution and pulse-shape discrimination ability (which allows to reduce background), CaMoO_4 scintillators could be considered as a promising tool in a ^{100}Mo $0\nu 2\beta$ experiment. To estimate sensitivity of the experiment, in the following we present calculations of some backgrounds from cosmogenic activities induced in CaMoO_4 crystals, as well as from internal pollution by the U/Th chains, and from two neutrino 2β decays of ^{100}Mo and ^{48}Ca . Natural composition of Ca and O, and 100% enrichment in ^{100}Mo is supposed.

Finite energy resolution of CaMoO_4 detector not only causes a broadening of ^{100}Mo $0\nu 2\beta$ peak, but also results in presence of events from tail of $2\nu 2\beta$ distribution in the peak's region. This background is unavoidable because it is caused by ^{100}Mo itself; it could be minimized only by improvement of the energy resolution of the detector. The response functions of CaMoO_4 scintillator for two neutrino and neutrinoless 2β decays of ^{100}Mo are presented in

Fig. 11 for 3%, 4%, 5% and 6% energy resolution (FWHM) of the detector at the energy of ^{100}Mo $0\nu 2\beta$ decay. Amplitude of $2\nu 2\beta$ ($0\nu 2\beta$) distribution corresponds to $T_{1/2}(2\nu) = 7 \times 10^{18}$ yr [24] ($T_{1/2}(0\nu) = 1 \times 10^{24}$ yr). It is evident from Fig. 11 that energy resolution should not be greater than 4–5%. For FWHM=4%, number of events from $2\nu 2\beta$ tail in 1 FWHM energy interval centered at $Q_{2\beta}$ is equal to 0.06 events per 1 kg of $\text{Ca}^{100}\text{MoO}_4$ crystal per 1 year.

Contribution from $2\nu 2\beta$ decay of ^{48}Ca could be much more dangerous (see Fig. 12). Measured half-life of this process is equal $T_{1/2}(2\nu) = 4 \times 10^{19}$ yr (see f.e. compilation [19]); ^{48}Ca is present in natural Ca composition with abundance of 0.187% [42]. Event's rate from ^{48}Ca $2\nu 2\beta$ decay in 1 FWHM energy interval is equal to 1.4 events per 1 kg of $\text{Ca}^{100}\text{MoO}_4$ crystal per 1 year.

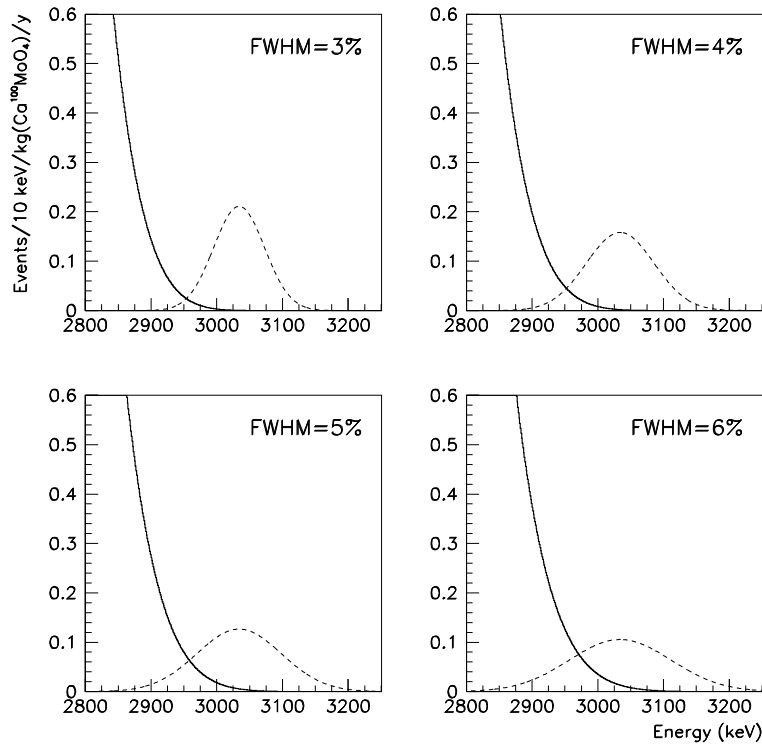


Fig. 11. The response functions of a $\text{Ca}^{100}\text{MoO}_4$ detector for 2β decays of ^{100}Mo for $T_{1/2}(2\nu) = 7 \times 10^{18}$ yr (solid lines) and $T_{1/2}(0\nu) = 1 \times 10^{24}$ yr (dashed lines) for different energy resolutions of the detector at the energy of ^{100}Mo $0\nu 2\beta$ decay.

In estimations of backgrounds from internal U/Th chains and cosmogenic activities, we additionally suppose use of an active shield made of CsI(Tl) scintillators. Radiopure CsI(Tl) scintillators were developed by the KIMS collaboration for the dark matter experiments in the Yangyang Laboratory [43]. In simulations, the CaMoO_4 crystal $\varnothing 45 \times 45$ mm was placed in the center of $\varnothing 40 \times 40$ cm CsI(Tl) scintillation detector. CaMoO_4 was viewed by two PMTs through light-guides also made of CsI(Tl)⁴. Such an active shield suppresses

⁴ Another possible solution could be light-guides made of PbWO_4 scintillators as

internal and external backgrounds related with emission of γ quanta. Contribution from cosmic ray particles in course of measurements could be effectively suppressed by deep underground location of the experiment.

Only two isotopes in U/Th chains have enough energy to create background in the region of $0\nu 2\beta$ peak of ^{100}Mo : ^{208}Tl ($Q_\beta=5001$ keV [39]) and ^{214}Bi ($Q_\beta=3272$ keV)⁵. Beta decay of ^{208}Tl is accompanied by emission of one or more γ quanta, and thus it is effectively eliminated by the CsI(Tl) active shield. Beta decay of ^{214}Bi is more dangerous because it has 18.2% branch to the ground state of ^{214}Po without emission of any γ 's and with $Q_\beta=3272$ keV. However, this contribution could be further suppressed by $\simeq 1$ order of magnitude by checking for fast α decay of ^{214}Po ($T_{1/2} = 164.3 \mu\text{s}$) during subsequent $\simeq 1$ ms and proving its α nature with the pulse-shape analysis. Contributions from ^{208}Tl and ^{214}Bi are shown in Fig. 12 for 0.1 mBq/kg activity. It is clear that they are not very dangerous in comparison with ^{48}Ca $2\nu 2\beta$ decay because comparative or even more clean CaMoO_4 crystals were already obtained (CMO-5 in Table 4: 0.04 mBq/kg for ^{208}Tl and 0.13 mBq/kg for ^{214}Bi).

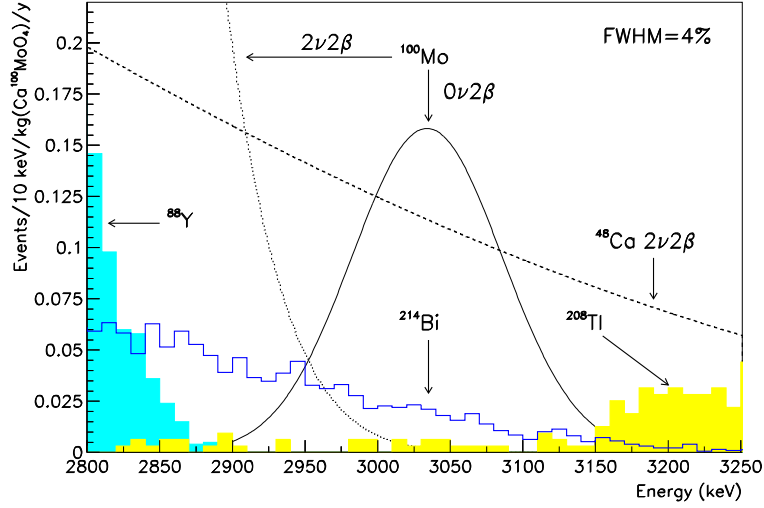


Fig. 12. Calculated backgrounds from $2\nu 2\beta$ decay of ^{48}Ca ($T_{1/2}(2\nu) = 4 \times 10^{19}$ yr), internal pollutions by ^{208}Tl and ^{214}Bi (both with 0.1 mBq/kg), and ^{88}Y isotope from cosmogenic activity. One order of magnitude suppression for ^{214}Bi with the pulse-shape analysis is taken into account. Amplitude of ^{88}Y distribution corresponds to 1000 decays in CaMoO_4 , much bigger than that expected from the ^{88}Y cosmogenic activity (4 events per year on average during the first 5 years). It is supposed that $\text{Ca}^{100}\text{MoO}_4$ scintillator is operating in anticoincidence with the CsI(Tl) active shield (see text). Distributions for ^{100}Mo are shown for $T_{1/2}(2\nu) = 7 \times 10^{18}$ yr and $T_{1/2}(0\nu) = 1 \times 10^{24}$ yr.

it was proposed in [44].

⁵ Formally also ^{210}Tl is present with $Q_\beta=5489$ keV but yield of this isotope in ^{238}U chain is only 0.021%.

Table 5

Cosmogenic radioactivity induced in $\text{Ca}^{100}\text{MoO}_4$ crystals. Exposition during 30 days to cosmic rays at the sea level and 1 yr period of cooling down in underground conditions are supposed. D_5 is number of decays during the first 5 years of data taking per 1 kg of the crystal.

Isotope or chain of decays	$T_{1/2}$	Decay mode and Q value		D_5
^{22}Na	2.6 yr	EC	2842 keV	8.99
^{42}Ar & ^{42}K	32.9 yr	β^-	3525 keV	0.80
^{56}Co	77.3 d	EC	4565 keV	0.01
^{60}Co	5.3 yr	β^-	2824 keV	2.08
^{68}Ge & ^{68}Ga	270.8 d	EC	2921 keV	0.90
^{88}Y	106.7 d	EC	3623 keV	20.69

Cosmogenic activities produced by cosmic rays in $\text{Ca}^{100}\text{MoO}_4$ crystal during its time production period at the Earth surface were calculated with the COSMO code [45]. An activation time of 30 days at sea level, and a deactivation time of 1 year underground were assumed. The most dangerous cosmogenic nuclides – with energy close or higher than $Q_{2\beta}$ of ^{100}Mo and noticeable yield – are summarized in Table 5. Simulations with GEANT4 [37] and initial kinematics given by the DECAY0 event generator [38] showed that contributions from cosmogenic activities are small in comparison with $2\nu 2\beta$ decay of ^{48}Ca (see Fig. 12 for ^{88}Y).

To estimate sensitivity of the experiment to ^{100}Mo $0\nu 2\beta$ decay in terms of half-life limit, we can use known formula: $\lim T_{1/2} = \ln 2 \cdot \eta \cdot N \cdot t / \lim S$, where η is the detection efficiency, N is the number of ^{100}Mo nuclei, t is the measuring time, and $\lim S$ is the maximum number of $0\nu 2\beta$ events which can be excluded with a given confidence level on the basis of the experimental data or simulated background. It is interesting to consider here only unremovable backgrounds from $2\nu 2\beta$ decays of ^{48}Ca and ^{100}Mo itself, neglecting all other external and internal backgrounds (which could be effectively suppressed by the active CsI(Tl) shield).

We will have 1.41 (0.06) events from $2\nu 2\beta$ decay of ^{48}Ca (^{100}Mo) in 1 kg $\text{Ca}^{100}\text{MoO}_4$ scintillator inside 1 FWHM interval centered at the ^{100}Mo $Q_{2\beta}$ energy during 1 year. In case of absence of other contributions, with measured 1 (or 2) events and expected background of 1.47 events, in accordance with the Feldman-Cousins procedure [46], value of $\lim S$ is equal to 2.9 (4.4) at 90% C.L. Taking into account that this interval contains 0.761 of the full ^{100}Mo $0\nu 2\beta$ peak, it gives half-life limit as: $T_{1/2}(0\nu) > 5.4 \times 10^{23}$ (3.5×10^{23}) yr. Thus, comparatively modest efforts with 1 kg crystal (which contains near

490 g of ^{100}Mo) and 1 yr measurement time could give an interesting $T_{1/2}$ limit which can be compared with the recent value from the NEMO-3 experiment: 4.6×10^{23} yr [24] obtained with 7 kg of ^{100}Mo after 389 d of data taking.

Final aim of the NEMO-3 experiment ($T_{1/2}(0\nu) > 2 \times 10^{24}$ yr) could be achieved with $\text{Ca}^{100}\text{MoO}_4$ scintillator at statistics of 10 kg·yr, i.e. also in a middle-scale experiment. However, further improvement will be difficult task: half-life limit of 10^{25} yr could be reached only at 200 kg·yr statistics. More sensitive searches for ^{100}Mo $0\nu 2\beta$ decay evidently will need in depletion of Ca in ^{48}Ca ⁶.

CaMoO_4 crystals could be also used as scintillating bolometers [16]. In this case energy resolution will be much better ($\simeq 5$ keV instead of $\simeq 120$ keV for 4%) that results in more clear interpretation of backgrounds and higher sensitivity of an experiment. Two neutrino 2β decay of ^{100}Mo will not contribute anymore to the $0\nu 2\beta$ peak. With background only from $2\nu 2\beta$ decay from non-depleted ^{48}Ca , the following half-life limits could be reached (at 90% C.L.): 6.5×10^{23} yr, 4.1×10^{24} yr, and 4.2×10^{25} yr for 1, 10 and 200 kg·yr statistics, respectively. Statistics of 1000 kg·yr would correspond to $T_{1/2}(0\nu) > 1.1 \times 10^{26}$ yr. In accordance with the NME calculations for ^{100}Mo $0\nu 2\beta$ decay [19,20], it will give limit on the effective neutrino mass in the range of 0.03–0.20 eV.

5 CONCLUSIONS

Scintillation properties and radioactive contamination of CaMoO_4 crystals produced by the Institute for Materials (Lviv, Ukraine), and by the Innovation Centre of Moscow Steel and Alloy Institute (Moscow, Russia) were studied.

The energy resolution 10.3%, 7.7%, and 4.7% for the 662, 1064, and 2615 keV γ lines was obtained with the CaMoO_4 sample of $\varnothing 38 \times 20$ mm produced by the Institute for Materials. To our knowledge, such an energy resolution was never reported for CaMoO_4 crystal scintillators.

The photoelectron yield of CaMoO_4 scintillator at room temperature was measured as 36% of CaWO_4 crystal, and $\approx 8\%$ of $\text{NaI}(\text{Tl})$.

The α/β ratio was measured with α particles of ^{241}Am α source, and by using α peaks from internal U/Th contamination. The dependence of the α/β ratio

⁶ Only 20 years ago, before the first laboratory observation of $2\nu 2\beta$ decay in 1987, it was difficult to imagine that this rarest observed in nature process could be a serious background in searches for more rare decays.

on energy of particles (E_α) in the energy interval 5–8 MeV can be described by the linear function $\alpha/\beta = 0.11(2) + 0.019(3)E_\alpha$.

Three components of scintillation decay ($\tau_i \approx 0.3 - 1, \approx 4$ and $\approx 17 \mu\text{s}$) and their intensities under α particles and γ quanta irradiation were measured by using transient digitizer with 20 MHz sampling frequency. It allows to discriminate α particles and γ quanta with reasonable efficiency.

The temperature dependence of light output and pulse shape were measured in the range of temperature $-158 \div +25 \text{ }^\circ\text{C}$ by recording the pulse shapes with subsequent off-line analysis. At the temperature of approximately $-50 \text{ }^\circ\text{C}$ the light output increases in ≈ 2 times comparatively to light output at room temperature. Averaged decay time increases with decreasing of temperature as $\langle\tau\rangle = 31.8(7) - 0.85(3)T + 0.0093(7) \times T^2$, where T is temperature in degree C. At the temperature $-50 \text{ }^\circ\text{C}$ (where the maximum of light output was observed) the averaged decay time for α particles of 5.25 MeV is $\approx 98 \mu\text{s}$. Temperature dependence of radioluminescence intensity of CaMoO_4 crystal was also investigated in the range of temperatures $-170 \div +40 \text{ }^\circ\text{C}$ with the help of photon counting method by averaging PMT counting rate over 10 s. It was found that light yield increases in ≈ 2.5 times at temperature $-80 \text{ }^\circ\text{C}$, and then remains practically unchanged at the further temperature decrease to $-170 \text{ }^\circ\text{C}$. We interpret such a difference in the behaviour of light yield on temperature measured by two methods as a result of very slow scintillation decay at temperatures lower than $\sim -50 \text{ }^\circ\text{C}$.

Radioactive contamination of CaMoO_4 crystals was estimated in low background measurements carried out in the Solotvina Underground Laboratory. CaMoO_4 scintillators produced in the Institute for Materials (Lviv, Ukraine) are considerably polluted by uranium and thorium (particularly by ^{210}Po at the level of $\approx 0.4 - 0.5 \text{ Bq/kg}$). The contamination of CaMoO_4 crystal produced by the Innovation Centre of the Moscow Steel and Alloy Institute (Moscow, Russia) is one–two order of magnitude better. It was found that equilibrium in uranium chains is broken in CaMoO_4 crystals. Some indication on increasing of radioactive contamination in the crystal volume during the growth process was observed.

Perspectives for a high sensitivity experiment to search for $0\nu 2\beta$ decay of ^{100}Mo are discussed. The energy resolution of 4–5% is enough to reach sensitivity at the level of 10^{25} yr . The contamination of crystals by ^{226}Ra and ^{232}Th should not exceed the level of 0.1 mBq/kg . Two neutrino mode of 2β decay of ^{48}Ca restricts sensitivity of an experiment to search for $0\nu 2\beta$ decay of ^{100}Mo with the help of CaMoO_4 crystal scintillators. A possible solution would be production of CaMoO_4 scintillators from Calcium depleted in ^{48}Ca . Further improvement of sensitivity could be reached by applying CaMoO_4 crystals as scintillating bolometers.

A R&D with aim to develop low-background, high resolution scintillation detector for an experiment to search for $0\nu 2\beta$ decay of ^{100}Mo with a sensitivity at the level of 10^{25} yr is in progress.

6 ACKNOWLEDGMENT

Work of A.N. Annenkov, O.A. Buzanov, V.N. Kornoukhov, M. Korzhik and O. Missevitch was supported in part by ISTC project #3293 in collaboration with the Dark Matter Research Center and School of Physics of Seoul National University, Republic of Korea.

References

- [1] F.A. Danevich et al., Instr. Exp. R. 32 (1989) 1059.
- [2] S.F. Burachas et al., Phys. Atom. Nucl. 58 (1995) 153.
- [3] F.A. Danevich et al., Z. Phys. A 355 (1996) 433.
- [4] P. Belli et al., Nucl. Phys. B 563 (1999) 97.
- [5] F.A. Danevich et al., Nucl. Phys. A 694 (2001) 375.
- [6] F.A. Danevich et al., Phys. Rev. C 68 (2003) 035501.
- [7] P. Belli et al., Nucl. Instr. Meth. A 498 (2003) 352.
- [8] I. Ogawa et al., Nucl. Phys. A 730 (2004) 215.
- [9] F.A. Danevich et al., Nucl. Instr. Meth. A 544 (2005) 553.
- [10] S. Belogurov et al., IEEE Nucl. Sci. 52 (2005) 1131;
H.J. Kim, et al., Proceedings of New View in Particle Physics (VIETNAM2004), August 5-11, 2004, p. 449.
- [11] V.B. Mikhailik et al., Phys. Stat. Sol. b 242 (2005) R17.
- [12] V.B. Mikhailik et al., J. Appl. Phys. 97 (2005) 083523.
- [13] V.B. Mikhailik et al., J. Phys.: Condens. Matter 17 (2005) 7209.
- [14] A. Senyshyn et al., Phys. Rev. B 73 (2006) 014104.
- [15] V.B. Mikhailik and H. Kraus, J. Phys. D: Appl. Phys. 39 (2006) 1181.
- [16] S. Pirro et al., Phys. Atom. Nucl. 69 (2006) 2109.
- [17] M. Doi et al., Prog. Theor. Phys. Suppl. 83 (1985) 1.

- [18] J. Suhonen and O. Civitarese, *Phys. Rep.* 300 (1998) 123.
- [19] V.I. Tretyak and Yu.G. Zdesenko, *At. Data Nucl. Data Tables* 61 (1995) 43; 80 (2002) 83.
- [20] F. Simkovic et al., *Phys. Rev. C* 64 (2001) 035501;
S. Stoica and V.P. Paun, *Rom. Journ. Phys.* 47 (2002) 497;
J. Suhonen, *Nucl. Phys. A* 700 (2002) 649;
O. Civitarese and J. Suhonen, *Nucl. Phys. A* 729 (2003) 867;
V.A. Rodin et al., *Phys. Rev. C* 68 (2003) 044302;
V.A. Rodin et al., *Nucl. Phys. A* 766 (2006) 107; erratum arXiv: 0706.4304v1 [nucl-th].
- [21] G. Pantis et al., *Phys. Rev. C* 53 (1996) 695.
- [22] Yu.G. Zdesenko et al., *Astropart. Phys.* 23 (2005) 249.
- [23] S.I. Vasil'ev et al., *JETP Lett.* 51 (1990) 622;
H. Ejiri et al., *Phys. Lett. B* 258 (1991) 17;
D. Dassie et al., *Phys. Rev. D* 51 (1995) 2090;
M. Alston-Garnjost et al., *Phys. Rev. C* 55 (1997) 474;
A. De Silva et al., *Phys. Rev. C* 56 (1997) 2451;
V.D. Ashitkov et al., *JETP Letters* 74 (2001) 529.
- [24] R. Arnold et al., *Phys. Rev. Lett.* 95 (2005) 182302.
- [25] H. Hidaka, C.V. Ly, K. Suzuki, *Phys. Rev. C* 70 (2004) 025501.
- [26] A.S. Barabash et al., *Phys. Lett. B* 345 (1995) 408;
A.S. Barabash et al., *Phys. At. Nucl.* 62 (1999) 2039;
M.J. Hornish et al., *Phys. Rev. C* 74 (2006) 044314;
R. Arnold et al. (NEMO Collaboration), *Nucl. Phys. A* 781 (2006) 209.
- [27] Yu.G. Zdesenko et al., *Nucl. Instrum. Meth. A* 538 (2005) 657.
- [28] T. Fazzini et al., *Nucl. Instrum. Meth. A* 410 (1998) 213.
- [29] F.A. Danevich et al., *Phys. Rev. C* 67 (2003) 014310.
- [30] E. Gatti and F. De Martini, *Nuclear Electronics* 2, IAEA, Vienna, 1962, p. 265.
- [31] L. Bardelli et al., *Nucl. Instr. Meth. A* 569 (2006) 742.
- [32] F.A. Danevich et al., *Nucl. Instr. Meth. A* 541 (2005) 583.
- [33] P. Belli et al., *Nucl. Phys. A* 789 (2007) 15.
- [34] L. Bardelli et al., arXiv:nucl-ex[0706.2422].
- [35] Yu.G. Zdesenko et al., *Proc. 2nd Int. Symp. Underground Physics, Baksan Valley, USSR, August 17–19, 1987. – Moscow, Nauka, 1988, p. 291.*
- [36] F.A. Danevich et al., *Phys. Lett. B* 344 (1995) 72.

- [37] S. Agostinelli et al., Nucl. Instr. Meth. A 506 (2003) 250;
J. Allison et al., IEEE Trans. Nucl. Sci. 53 (2006) 270.
- [38] O.A. Ponkratenko, V.I. Tretyak, Yu.G. Zdesenko, Phys. At. Nucl. 63 (2000) 1282; V.I. Tretyak, to be published.
- [39] R.B. Firestone et al., *Table of Isotopes*, 8th ed., John Wiley & Sons, New York, 1996 and CD update, 1998.
- [40] A.Sh. Georgadze et al., Instrum. Exp. Tech. 39 (1996) 191.
- [41] S.Ph. Burachas et al., Nucl. Instr. Meth. A 369 (1996) 164.
- [42] J.K. Bohlke et al., J. Phys. Chem. Ref. Data 34 (2005) 57.
- [43] H.S. Lee et al., Phys. Lett. B 633 (2006) 201;
H.S. Lee et al., Nucl. Instr. Meth. A 571 (2007) 644.
- [44] F.A. Danevich et al., Nucl. Instr. Meth. A 556 (2006) 259.
- [45] C.J. Martoff and P.D. Lewin, Comp. Phys. Comm. 72 (1992) 96.
- [46] G.J. Feldman and R.D. Cousins, Phys. Rev. D 57 (1998) 3873.